Erschienen in: Energy Procedia ; 92 (2016). - S. 75-81
https://dx.doi.org/10.1016/j.egypro.2016.07.018

Available online at www.sciencedirect.com

ScienceDirect

Energy Procedia 92 (2016) 75 – 81

Energy Procedia

6th International Conference on Silicon Photovoltaics, SiliconPV 2016

Finite element simulation of the local Al/Si contact formation

Axel Herguth

University of Konstanz, Department of Physics, 78457 Konstanz, Germany

Abstract

The formation of local Al/Si contacts, as found in PERC type cells, was evaluated by finite element simulation based on a model of Si diffusion in the molten Al layer as well as dissolution and recrystallization of Si at the liquid/solid interface. In accordance with experimental observations the simulations reproduce the characteristic lateral spread of Si in the Al layer, the different cavity shapes (ranging from round to ω-shaped cavities) as well as the development of the Al-doped recrystallized region which forms the high-low junction to the lower doped substrate responsible for the back surface field passivation.

© 2016 The Authors. Published by Elsevier Ltd. This is an open access article under the CC BY-NC-ND license (http://creativecommons.org/licenses/by-nc-nd/4.0/).
Peer review by the scientific conference committee of SiliconPV 2016 under responsibility of PSE AG.

Keywords: Al/Si contact formation; local contacts; PERC

1. Introduction

Nowadays, most industrially manufactured silicon solar cells still feature a virtually one-dimensional layered structure consisting of full area n^+-emitter on top of a p-type substrate and a full area back contact realized by alloying screen-printed Al with Si from the substrate. Within this alloying process, a strongly Al-doped (sometimes also B-codoped) region evolves forming a high-low junction. The resulting electrical back surface field (BSF) repels electrons thus reduces the electron concentration at the physical Si/metal interface and in consequence lowers recombination activity there. Even though this concept provides a decent passivation within a technological simple, robust and economic process, it hampers further improvement of solar cell conversion efficiency beyond 20%.

With the introduction of PERC type concepts (passivated emitter and rear cell) the full area Al/Si rear contact is replaced by local Al/Si contacts which form in openings of the otherwise dielectrically passivated back side. This refined passivation improves the efficiency potential well beyond 22%. However, even though contact formation in local openings still results in a 'local' BSF, the different geometry changes the alloying process in some details.

Within this contribution, the dynamics of Si dissolution, diffusion, and recrystallization is studied by simulations to assess the otherwise hardly accessible temporal evolution of the contact and to evaluate the role of geometrical constraints like Al layer thickness and opening width in the otherwise impermeable dielectric layer.

Konstanzer Online-Publikations-System (KOPS)
URL: http://nbn-resolving.de/urn:nbn:de:bsz:352-0-373248

1876-6102 © 2016 The Authors. Published by Elsevier Ltd. This is an open access article under the CC BY-NC-ND license (http://creativecommons.org/licenses/by-nc-nd/4.0/).
Peer review by the scientific conference committee of SiliconPV 2016 under responsibility of PSE AG.
doi:10.1016/j.egypro.2016.07.018

2. The Al/Si phase diagram in and out of equilibrium

For the understanding of the simulations, it is essential to understand some of the properties of the Al/Si alloying process. In Fig. 1 the binary Al/Si phase diagram is given. For the alloying process itself, the left hand part with low silicon fractions is important. For the incorporation of Al as dopant into the Si matrix, the right hand part is relevant.

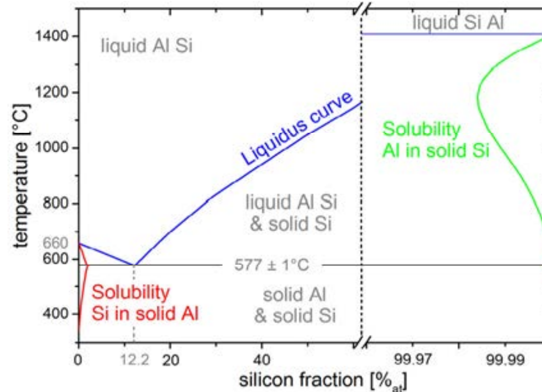

Fig. 1. Binary phase diagram of Al and Si in equilibrium including the melting point of pure Al (~660°C), the eutectic solidification point (~577°C, ~12.2%), and the solubility curves of Si in liquid Al (blue), Si in solid Al (red) and vice versa Al in solid Si (green). after [1].

From the phase diagram it can be seen that pure Al melts at around 660°C. In principle, Si pre-contaminated Al melts at lower temperatures. An unsolved question is how much Si already diffuses into the solid Al before a temperature of ~660°C is reached and if this means that there is an interlayer already melting below 660°C. Fortunately this solid state diffusion does not seem to be very pronounced and is therefore excluded from the suimulations.

The phase diagram is explicitly valid only in equilibrium thus means it is only applicable globally for an evenly intermixed situation as maybe found in mixed powders. In a situation as found in a solar cell with a relatively thick Al layer on top of a Si substrate, equilibrium is, strictly speaking, found only at the interface. Thus the (infinitely thin) interface layer follows perfectly the blue Liquidus line in Fig. 1. If solubility of Si in the Al melt increases with rising temperature, Si is dissolved from the adjacent solid and the interface becomes the melting front. If solubility decreases with falling temperature, Si recrystallizes and the interface becomes the crystallization front.

At every other position in the Al melt other than the interface layer, the system tries to relax towards equilibrium. In a region with too less Si solved in the Al melt Si tries to accumulate but as no Si is available, the Al melt is chronically under-saturated. This means, e.g., that at 800°C locally only a silicon fraction of 10% can be present, even though ~27% could be solved, a point far within the liquid Al phase in Fig. 1. Dissolving new Si, e.g., from a Si particle, is, however, not allowed as this would yield an interface layer.

In principle it is also possible that the system becomes locally super-saturated, e.g., by cooling and decreasing solubility. In an effort to relax to equilibrium, Si will try to crystallize but, as there is no seed (surrounded by a crystallization front), fails to do so. Spontaneous seeding and precipitation of Si will, however, set in if the super-saturation becomes too strong. Spontaneous seeding is not included in the simulations.

In summary, the phase diagram only describes properly the situation in the interface layer in between liquid Al and solid Si. Further away, the Al melt is more likely either under- or super-saturated. This also means that there exists almost always a Si concentration gradient (either away from or towards) between interface layer and Al melt that will drive a diffusion of Si into or out of the melt. In addition there will be also a gradient in the Al melt responsible for redistribution in the melt trying to equilibrate the whole system.

Incorporation of Al into the layer-by-layer recrystallized Si, being the main goal of the alloying process, is governed by the Al solubility in solid Si at the temperature a layer crystallizes at. The same accounts for B as possible co-dopant as well.

3. Simulation constraints

As described in the previous section, (local) Al/Si contact formation is mainly driven by Si dissolution and recrystallization in combination with a gradient-driven diffusion in and out of the Al melt at the interface and within the Al melt itself. This, of course, holds also for non-local contact formation, but the implications are by far more pronounced for the local case.

A typical PERC-like rear contact pattern comprises of a set of uninterrupted parallel lines with a pitch distance of around 1 mm. The exact value used in reality may deviate according to substrate doping or other constraints. The opening width varies from extremely small (~10 µm) to extremely wide (~100 µm). The Al layer thickness varies from a few microns (~5 µm for evaporated Al) to 25 µm (for screen printed pastes). The chosen two-dimensional simulation domain, lying perpendicular to the contact line, is limited to a symmetry element comprising laterally of half the pitch distance of the local openings (0.5 mm) and in depth Al layer thickness (5-15 µm) plus as much as is necessary of the Si substrate to allow complete cavity formation. A symmetry line is located in the center of the opening in the dielectric passivation layer. The passivation layer is chosen relatively thick with 400 nm for better visualization. A significant impact of such a thick dielectric layer is not expected regarding the overall dimensions of the simulation domain. For aesthetic visualization issues the domain is mirrored at the symmetry line.

All investigations are based on a diffusion based model implemented in a finite element framework (written in MatLab) allowing to track dynamics in time and 2D-space. Within this model Si is dissolved from the solid Si substrate into the liquid Al phase, diffuses according to Fick's laws and eventually recrystallizes. Dissolution and recrystallization are governed by temperature dependent solubility of Si in the liquid Al phase according to the phase diagram shown in Fig. 1. Diffusion is controlled by temperature dependent diffusivity of Si in the liquid Al phase according to an Arrhenius law using an activation energy of 1.41 eV and an exponential prefactor of ~2 cm²/s as found in literature. As these values did not match the values found for Al screen-printing pastes [2] for unknown reasons, an enhancement factor of 5 was used within the simulations presented here. This yields, e.g., an enhanced diffusivity around $2.5 \cdot 10^{-6}$ cm²/s at 800°C. However, as the simulations presented here shall demonstrate the different effects at work, and as the diffusivity of Si in screen-printed Al-pastes differs by roughly an order of magnitude, the system simulated here has to be considered an idealized model system.

The temperature profile shown in Fig. 2 was used for the simulations. The temperature range, in which the alloying process takes place, is marked in red and is limited by the melting of the Al layer at 660°C and the final recrystallization at the eutectic temperature of 577°C. Even though temperature is in principle not only variable in time, it is at this point kept fixed in space. This corresponds to the assumption of a slow temperature change, when temperature can equilibrate at any time in the whole simulation domain and melting/crystallization heat is negligible or buffered by the rather large heat capacity of the comparably thick substrate in combination with a high heat conductivity of silicon.

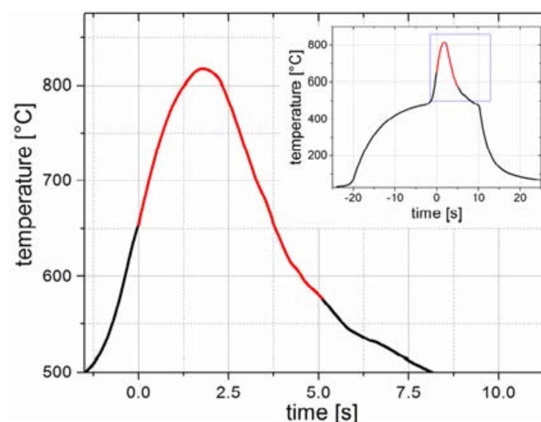

Fig. 2. Typical firing profile (inset) used for screen-printed solar cells. The temperature profile used for the simulations is marked in red and comprises of the temperature range when pure and Si enriched Al is molten.

4. Results

4.1. Temporal evolution

In Fig. 3 the temporal evolution of the Si concentration in the molten Al layer is shown.

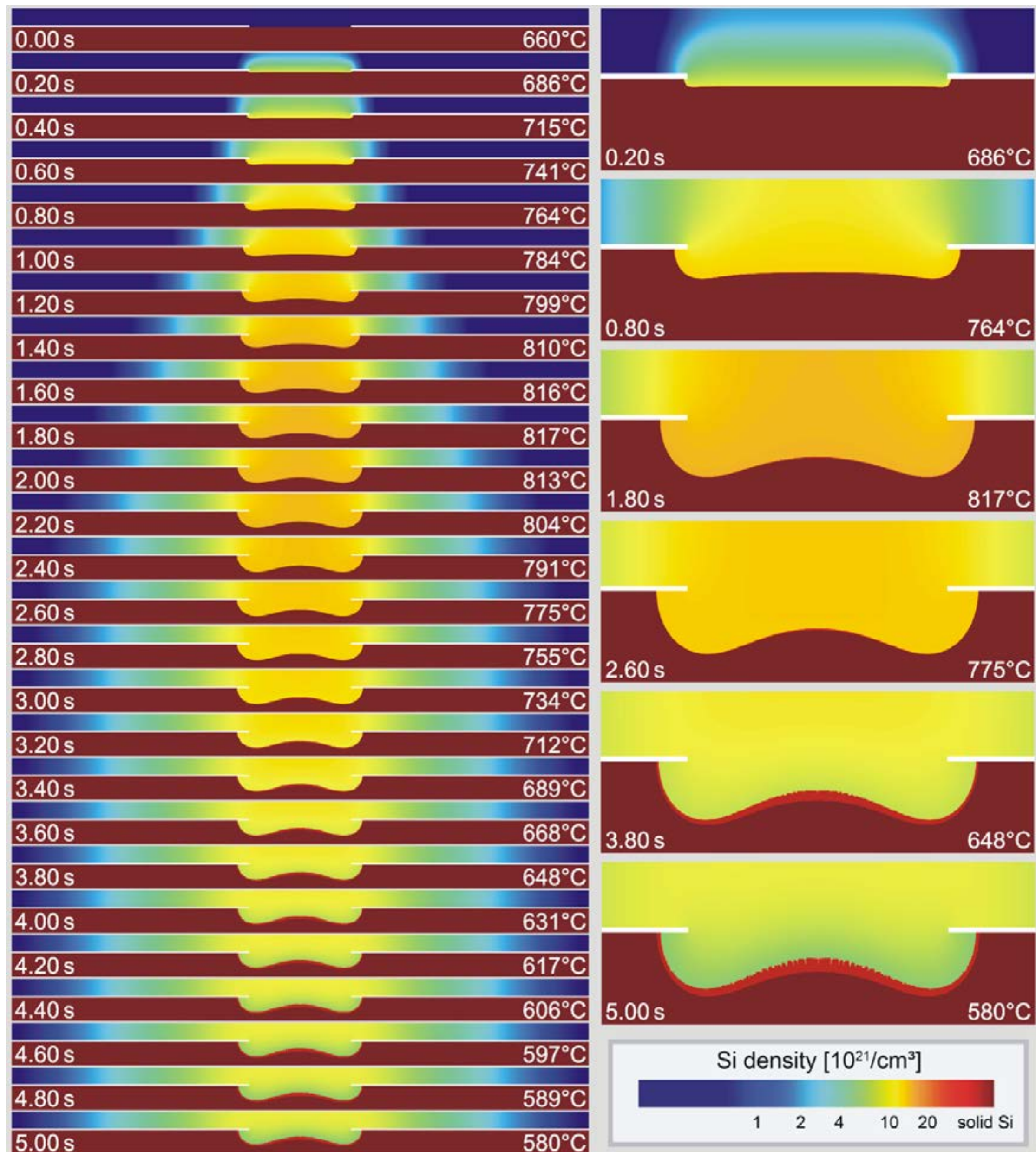

Fig. 3. Concentration images in the cause of time showing the lateral spread of Si due to diffusion in the molten Al layer (5 µm, initially Si lean, deep blue) on top of the solid Si substrate (deep red). A dielectric layer (0.4 µm, white), being impermeable for Si, separates Al layer and Si solid except for an opening of 30 µm in the centre. An ω-shaped cavity develops by Si dissolution from the solid Si which is later on (>2.60 s passed) partially filled by recrystallization (bright red layer in the cavity).

In the very beginning, diffusion of the freshly dissolved silicon occurs along the vertical axis, horizontal diffusion is negligible. A cavity begins to form vertically. As the diffusion front reaches the surface of the molten Al layer, the vertical concentration gradient in the centre begins to flatten out and the originally two-dimensional diffusion turns into one-dimensional lateral diffusion. Due to the weakened concentration gradient in the centre of the opening the dissolution of new Si from the solid is reduced while the stronger gradient at the opening edges leads to stronger dissolution and Si drainage. In consequence, pockets begin to deepen at the cavity edges undercutting the dielectric layer and an ω-shaped cavity forms. Note that the cavity shape depends on the geometric constraints as will be illustrated in section 4.3.

Maximal extension of the cavity is reached at around 2.60 s well after the maximum temperature has passed (at ~1.74 s). Up to that point, no recrystallization has occurred even though the temperature and thus solubility in the interface layer is already falling. This recrystallization delay is caused by the steady drainage of Si from the cavity due to lateral out-diffusion. At around 2.60 s the lowered diffusivity of Si in the molten Al hampers further out-diffusion to such an extent so that the interface layer concentration falls below the concentration in the cavity and the gradient reverses now driving Si back to the interface instead of away from it. This marks the time at which recrystallization finally starts. Note that the melt in the cavity is now super-saturated, a mandatory prerequisite for the gradient reversal. Also around 2.60 s lateral spread is almost complete. Even though there is still a lateral gradient in effect, the decreasing diffusivity limits further spread.

During further cooldown, a recrystallized Si region forms layer-by-layer meanwhile incorporating Al. Recrystallization generally depletes the Al melt but, as diffusivity of Si in the molten Al decreases rapidly, depletion is limited only to the adjacent region. The Si concentration in the still molten Al layer remains rather untouched, or in other words, plenty of Si, having diffused to far from the cavity, does not return. In this specific simulation, a fine structure in the recrystallized region occurs. This is most probably an artefact, however, the strongly reduced diffusivity at low temperatures in the end phase promotes such spike-like instabilities as crystallization at exposed sites is physically favoured and often observed in other systems.

Finally the melt solidifies at around 577°C which is explicitly not shown in the simulation. In the attempt to reach the eutectic point (see Fig. 1), Si will spontaneously precipitate from the super-saturated melt probably forming the lamella shaped Si inclusions often found in the resolidified Al layer above the cavity. Once the eutectic point is reached, the melt breaks up Al and Si lamellas form as there exists no common Al/Si solid phase despite the rather small solubilities (red and green lines in Fig. 1). This, however, is not to be mixed up with the recrystallized region during cool down having incorporated larger amounts of Al at higher temperatures.

Voids (empty cavities) cannot form within the framework of this simulation, as it requires an adhesion breakdown of the liquid/solid interface and subsequent retraction of Al melt from the cavity and Al motion is simply not part of this simulation. However, up to the point of adhesion breakdown the simulation remains valid.

4.2. Gradient analysis

From the images shown in Fig. 3, Si concentration profiles along certain lines can be extracted. In Fig.4a this is done for characteristic times along the central mirror axis located in the middle of the cavity. As can be seen from the hard step in concentration of Si in the Al melt, the interface moves during the dissolution phase deeper into the solid silicon (shift to the right) and later on, in the recrystallization phase, back into the direction of the former Si surface. Maybe in contrast to Fig. 3, the changing gradient can be seen more clearly. In the dissolution phase lasting approx. until 2.60 s, the concentration profile features a convex shape meaning a gradient driving Si from the interface layer into the melt. As long as this convex shape is maintained during cooling, recrystallization cannot take place as the interface layer is steadily depleted of Si.

Only after the concentration profile becomes concave at around 2.60 s, Si is driven back to the interface layer and melting front turns into crystallization front. The concave shape becomes more pronounced the colder the system gets. However, even though the overall level near the Al surface decreases, only the direct surroundings of the crystallization front are seriously depleted. In other words, Si having diffused too far into the Al layer is trapped there due to the steadily decreasing diffusivity with falling temperature and plenty of Si is therefore lost for recrystallization.

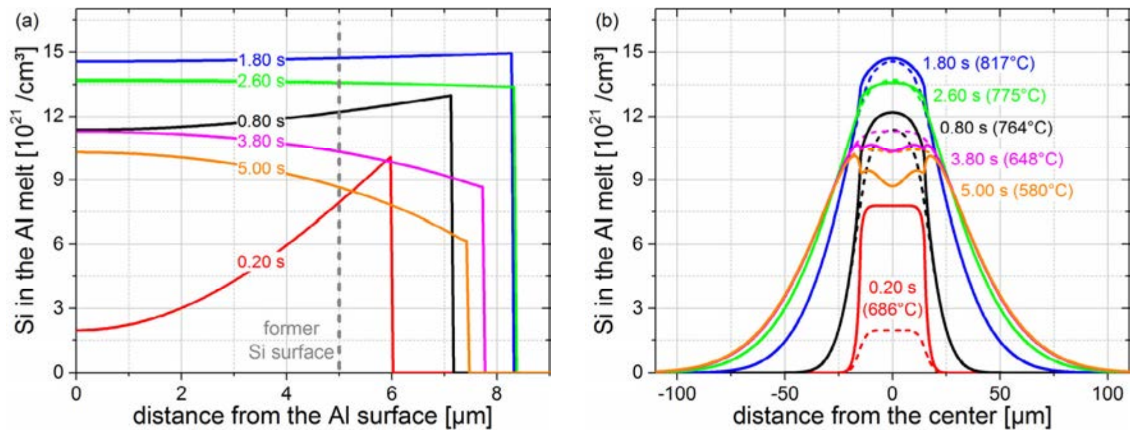

Fig. 4. Si concentration profiles along the vertical central axis (a) and along horizontal lines (b) close to the dielectric layer (solid lines) and close to the Al surface (dashed lines) for selected times. (a) The vertical cut illustrates the deepening of the cavity due to dissolution (until 2.60 s) and its subsequent partial filling due to recrystallization. The profile shape changes at that time from convex to concave. (b) The horizontal cuts show the lateral spread of Si due to diffusion as well as the depletion of the cavity region during the crystallization visible being from the gap in between the solid and dashed line for 3.80 s and 5.00 s.

Fig. 4b shows the Si concentration in the melt close to the Al surface (dashed lines) and close to the dielectric layer (solid lines) as well. The 2D diffusion in the beginning can be seen from the huge difference between the red curves extracted at 0.2 s. Si simply had not enough time to penetrate to the Al surface. The lateral spread of Si increases with time but the main contribution to lateral spread occurs in between the black line (764°C) and the green line (775°C). This is the phase when diffusivity is rather high but ascribing the spread only to the phase of highest temperature is too simple an assumption leading to erroneously determined diffusivities. Beyond 2.60 s lateral spread virtually ceases. However, this is not the case in the cavity region. In contrast to the beginning (red lines), the concentration near the dielectric layer (solid lines) drops behind those found near the Al surface (dashed lines), which is also visible in Fig. 4a, indicating the stronger depletion of Si in the Al melt closer to the interface layer. In the end phase (3.80 s and 5.00 s) there exists a veritable gap in between dashed and solid lines.

4.3. Cavity shaping

In Fig. 5 it is shown that the shape of the cavity depends on the geometrical constraints. A rather round cavity forms if the Al layer is thick compared to the opening in the dielectric layer. With the subsequent widening of the opening while maintaining the Al layer thickness, the cavity bottom flattens and finally turns into an ω-shape.

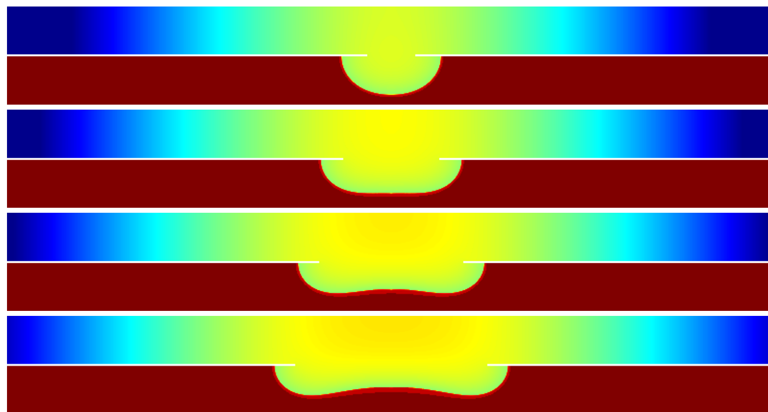

Fig. 5. Cavity shapes developed after the firing process for a 10 µm thick Al layer with varying opening width in the dielectric layer (top to bottom:10 µm, 20 µm, 30 µm, 40 µm).

5. Conclusions

The simulations illustrate the formation of the cavity in local Al/Si contacts, as found in PERC type cells, during the firing step including the lateral spread of Si in the Al layer as well as the recrystallization of the stronger Al-doped region which forms the desired high-low junction to the lower doped substrate. The simulations also allow for a time resolved analysis, which seems hardly possible in reality. As seen from the temporal evolution (Fig. 3), recrystallization does not start at maximum temperature, but is delayed due to the continuous drainage of the interface layer into the initially chronically under-saturated melt in the cavity. The recrystallization begins only after the gradient reverses which requires mandatorily super-saturation of the Al melt. The shape of the cavity depends on both Al layer thickness and opening width in the dielectric layer.

References

[1] Murray JL, McAlister AJ. The Al-Si system. Bulletin of Alloy Phase Diagrams, 1984:5(1):74-84

[2] Lauermann T, Fröhlich B, Hahn G, Terheiden B. Diffusion-based model of local Al back surface field formation for industrial passivated emitter and rear cell solar cells. Progress in Photovoltaics: Research and Application 2015:23(1):10-18